

ENERGETICS OF THE BASIC ALLOTROPES OF CARBON

ABSTRACT

An effort was made in this work to calculate the total ground state energy and electronic band structure of Fullerenes (C_{60}), Graphite and Diamond using FHI-aims Density Functional Theory (DFT) code. The density functionals used are the local-density approximation (LDA) in the parameterization by Perdew and Wang 1992, Perdew and Zunger 1981, the generalized gradient functional PBE, and PBE+vdW approach as defined by Tkatchenko and Scheffler. The results obtained from the computations of the ground state energies of diamond, fullerenes and graphite were -2072.569 eV, -1027.178 eV and -2070.938 eV respectively. These results agrees well when compared to the various exchange and correlation functionals used in this study. Similarly, the results obtained from the computations of the Kohn Sham electronic band gaps of graphite and diamond were 0.00072eV and 5.57611eV, respectively. These are also in agreement when compared to the experimental values of 0eV and 5.45eV. These band gaps are within reasonable percentage errors of 0.0% and 1.43% respectively. However, fullerenes band gap of 8.21131eV is not in agreement with the theoretical and experimental values of 1.83eV and 2.3eV, respectively. This is probably due to the Bucky-ball nature of Fullerenes as well as the lattice constants and physical settings used.

Keywords: DFT, LDA, GGA, Band Gap, HOMO, LUMO and Total Ground state Energy.

1. INTRODUCTION

Carbon is found naturally in the earth crust and in the atmosphere. It is abundant and forms a major part of our life. Carbon is a unique and versatile element. It exists in many forms with different structures and properties. It can also be synthesized to form new forms of materials [1]. Carbon is the basic building block of the following Carbon materials: graphite, diamond, fullerene, graphene, Carbon-fiber, Carbon nanotube, lonsdaleite, carbyne and buckydiamonds. Recently, new Carbon forms penta-graphene [2] and novamene [3] were discovered. The ability of Carbon to exist in many

19 forms with different structures and properties led researchers into a rigorous research on Carbon
20 nanomaterial.

21 The principal allotropes of Carbon are graphite, diamond and Fullerenes. Diamond is associated with
22 the sp^3 hybrid orbital, all four electrons are used to form a tetravalent sigma σ bond in a 3D structure.
23 In each unit cell, diamond has eight Carbon atoms. The bond length is equidistant between the four
24 Carbon atoms, thereby forming a strong covalent bond with bond angle of 109.5° . Diamond is the
25 hardest known material, it is used in cutting, drilling and grinding. It is transparent in the visible range
26 of the electromagnetic spectrum, making it a good candidate for jewelry. It has a high thermal
27 conductivity (more than copper) and low thermal expansion [1 and 4]

28 Graphite has a flat layered (planar) structure. Each Carbon atom forms trivalent (sigma σ) bond with
29 three (sp^2 hybrid orbital) other Carbon atoms in a hexagonal shape which are arranged to form a
30 layer. The layers are bonded to one another by weak Van-der-Waal forces. This allows the layers to
31 slip over each other. The p_z – orbitals electrons, do also interact: they form a π -mobile electron.
32 Graphite is the most stable and most strongly covalently bonded Carbon allotrope (within the layer). It
33 is soft, opaque, black, used in pencil, lubrication and in nuclear reactor moderator [1 and 4].

34 In recent time, a new Carbon allotrope was discovered by Curl, Kroto and Smalley at Rice University.
35 It is spherical (soccer ball) in shape. It resembles a geodesic dome constructed by an architect in
36 person of Richard Buckminster Fuller. Hence, it was named in his honour as buckminsterfullerene,
37 shortened as fullerenes (also called buckyballs). It has sixty (60) Carbon atoms arranged in both
38 pentagonal and hexagonal shape. For it to have a spherical shape, it must satisfy the pentagon rule
39 i.e. it must have 12 pentagons and 20 hexagons. Basic Fullerene molecular formula is C_{60} [1 and 4].
40 Unlike graphite and diamond, fullerene molecule has both sp^3 and sp^2 hybrid orbitals, i.e., It has both
41 sigma and pi bond. Fullerene is used as a high temperature superconductor when doped with K or
42 Rb, it is a possible lubricating aid and is also used in medicine [1 and 5].

43 Nowadays, Density Functional Theory (DFT) is one of the leading tools used in studying the electronic
44 structure, stability, synthesis, defects, semiconducting and superconducting properties of Carbon
45 materials. DFT is a special computational quantum mechanical first principle method of describing
46 and predicting the electronic structures and properties of atoms, molecules and solids.

47 In this work, using FHI-aims DFT package [6] structural units of Carbon basic allotropes were
48 simulated.

49 2. MATERIAL AND METHODS

50 First principles, or *ab initio* calculations represent the pinnacle of electronic structure calculations.

51 Starting with the fundamental constants and Schrodinger's equation as a postulate, these methods
52 proceed to describe the nature of atomistic systems to a degree that is almost irrefutable. The
53 methods applied in solving Schrodinger's equation break into two main types: Hartree-Fock (HF)
54 based methods and Density Functional Theory (DFT) methods. While both make approximations to
55 make calculations possible, they represent the best available methods for atomistic modeling. The
56 first task is to have a Linux based operating system (OS) (Ubuntu 16.04 version installed for this
57 research work) on a computer. FHI-aims is not supported on windows. Since FHI-aims is distributed in
58 source code form, the next task is to compile a powerful executable program. For this, the following
59 mandatory prerequisites are needed [6]:

- 60 • A working FORTRAN compiler. A good example is Intel's ifort compiler.
- 61 • A compiled version of the lapack library, and a library providing optimized basic linear algebra
- 62 subroutines (BLAS). Standard commercial libraries such as Intel's mkl provide both lapack and BLAS
- 63 support. Having an optimized BLAS library for a specific computer system is critical for the
- 64 performance of FHI-aims.

65 FHI-aims requires two input files — control.in and geometry.in—located in the same directory from
66 where the FHI-aims binary is invoked. An output file contains the basic information and result of the
67 calculation such as the total energy, atomic forces, etc. The geometry.in file contains all information
68 concerning the atomic structure of the system. This includes the nuclear coordinates, which are
69 specified by the keyword atom, followed by Cartesian coordinates (in units of Å) and the descriptor of
70 the species [7]. The control.in file contains all other physical and technical settings for accurate and
71 efficient convergence of the computations.

72 The full algorithmic framework embodied in the FHI-aims computer program package is described in
73 [6]. The algorithms are based on numerically tabulated atom-centered orbitals (NAOs) to capture a
74 wide range of molecular and materials properties from quantum-mechanical first principles. An all-
75 electron / full-potential treatment that is both computationally efficient and accurate is achieved for

76 periodic and cluster geometries on equal footing, including relaxation and *ab initio* molecular
77 dynamics.

78 2.1 COMPUTATIONAL DETAILS

79 Various computations were done for the pw_lda, pz_lda and pbe XC functionals. The Gaussian
80 occupation broadening width of 0.01eV was selected. The convergence criterion for the SCF of
81 eigenvalues, total energy and density were set to 10^{-2} eV, 10^{-5} eV and 10^{-4} eV, respectively. The
82 structure geometry with a convergence minimum of 10^{-2} eV was optimized, while for the unit cell
83 geometry optimization we selected full unit cell relaxation option. The corresponding convergence
84 criteria for the SCF of the energy derivatives was chosen to be 10^{-4} eV.

85 Tier 1 basis functions of FHI-aims light species_default basis set was used for the geometry
86 optimization, however, tier 2 tight basis set was used for the post relaxation of the relaxed geometry.
87 BFGS (Broyden, Fletcher, Goldfarb and Shanno) structure optimization algorithm was selected for the
88 geometry relaxation. FHI-aims keyword k_grid was set to 12x12x12 k_grid data point. For the long
89 range correlation energy interaction effect, we used VdW correction based on Tkatchenko and
90 Scheffler long range interaction correction.

91 3. RESULTS

92 The following tables summarize the output data obtained during FHI-aims computations, and are used
93 in discussing the minimum and stable ground state energies for the relaxed/post relaxed
94 computations of the various XC functionals for the three bulk structures.

95 Table 4.1: Diamond Ground State Energies for Relaxed/Post Relaxed Computations.

Functionals Computations	Pw_lda Ground State Energy (eV)	Pz_lda Ground State Energy (eV)	Pbe (GGA) Ground State Energy (eV)
Relaxed Geometry (Light)	-2056.94097548	-2056.90780088	-2072.47722687
Postrelaxed Geometry (Tight)	-2057.03098622	-2056.99760599	-2072.56851605

96

97

98 Table 4.2: Graphite Ground State Energies for Relaxed/Post Relaxed Computations

Functionals Computations	Pw_Ida Ground State Energy (eV)	Pz_Ida Ground State Energy (eV)	Pbe (GGA) Ground State Energy (eV)
Relaxed Geometry (Light)	-2044.81236553	-2044.81251118	-2061.63381564
Postrelaxed Geometry (Tight)	-2054.61937938	-2054.63065901	-2070.93836837

99

100 Table 4.3: Fullerenes Ground State Energies for Light and Tight Settings.

Functionals Computations	Pw_Ida Ground State Energy (eV)	Pz_Ida Ground State Energy (eV)	Pbe (GGA) Ground State Energy (eV)
Light	-1018.35981067	-1018.35683745	-1027.17026568
Tight	-1018.36680612	-1018.36379535	-1027.17849607

101

102 Table 4.4: Diamond Electronic Band Structure for Postrelaxed Computations

Functionals Bands	Pw_Ida Ground State Energy (eV)	Pz_Ida Ground State Energy (eV)	Pbe (GGA) Ground State Energy (eV)
Valence Band Maxima (VBM)	-8.54310497	-8.53387243	-8.10988403
Conduction Band Minima (CBM)	-4.34300078	-4.34356041	-3.95778618
HOMO-LUMO Gap	4.20010419	4.19031201	4.15209785
Smallest Direct Gap	5.61457427	5.60711319	5.57611325

103

104 Table 4.5: Graphite Electronic Band Structure for Postrelaxed Computations

Functionals	Pw_Ida Ground State Energy (eV)	Pz_Ida Ground State Energy (eV)	Pbe (GGA) Ground State Energy (eV)

Bands			
Valence Band Maxima (VBM)	-7.07415413	-7.33934792	-6.81313445
Conduction Band Minima (CBM)	-7.06569011	-7.33861834	-6.80852692
HOMO-LUMO Gap	0.00846402	0.00072958	0.00460753
Smallest Direct Gap	0.21308645	0.41541884	0.30724683

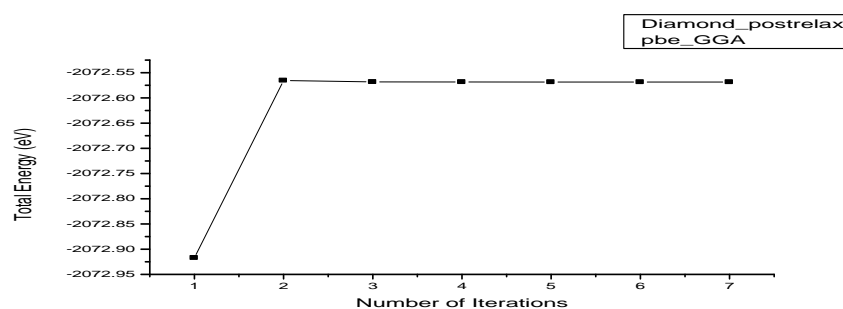
105

106 Table 4.6: Fullerenes Electronic Band Structure for Tight Settings Computations

Functionals	Pw_Ide Ground State Energy (eV)	Pz_Ide Ground State Energy (eV)	Pbe (GGA) Ground State Energy (eV)
Valence Band Maxima (VBM)	-13.60248641	-13.60706560	-13.71228408
Conduction Band Minima (CBM)	-5.39117210	-5.39539613	-5.25904269
HOMO-LUMO Gap	8.21131431	8.21166947	8.45324138
Smallest Direct Gap	8.21131432	8.21166948	8.45324139

107

108 The following graphs summarize the output data obtained during FHI-aims computations, and are
 109 used in obtaining the binding curve pattern for the total energy and the number of iterations.



110

111 Fig. 4.1: Variations of Total Energy (eV) against Number of Iterations

112

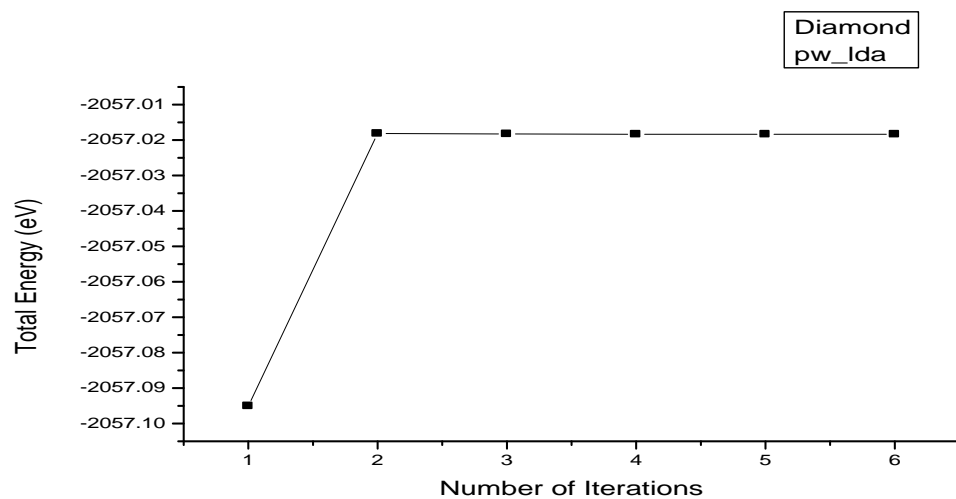


Fig. 4.2: Variations of Total Energy (eV) against Number of Iterations.

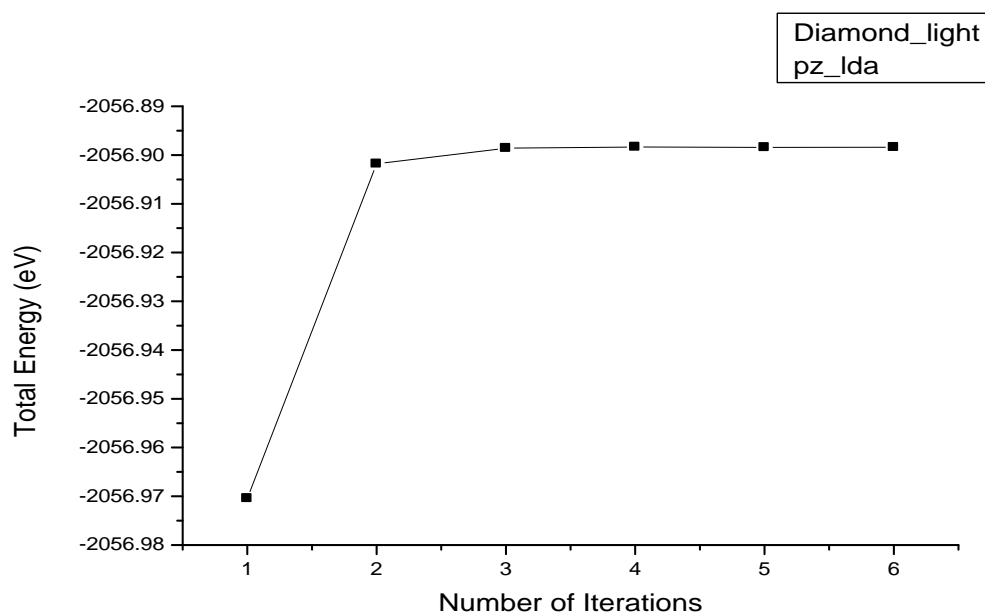


Fig. 4.3: Variations of Total Energy (eV) against Number of Iterations.

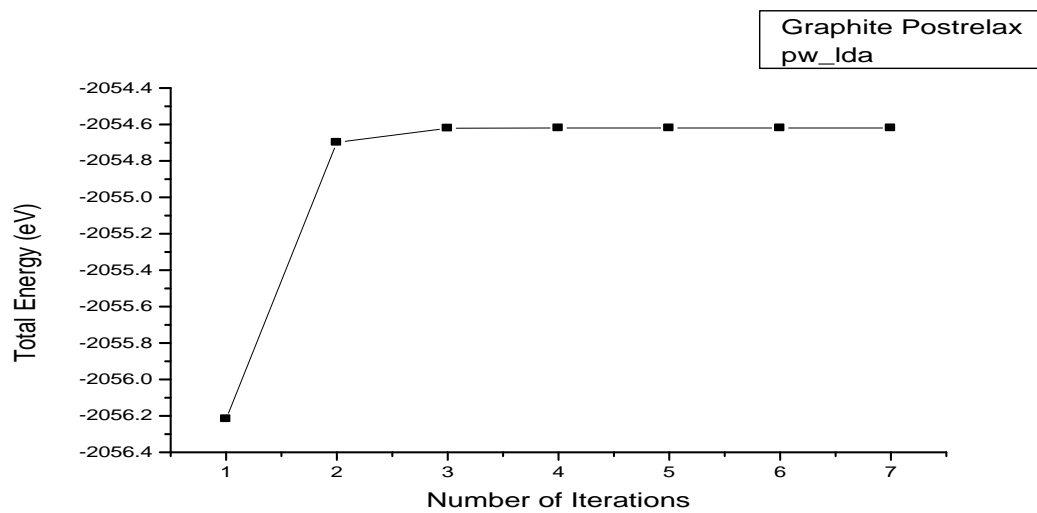


Fig. 4.4: Variations of Total Energy (eV) against Number of Iterations.

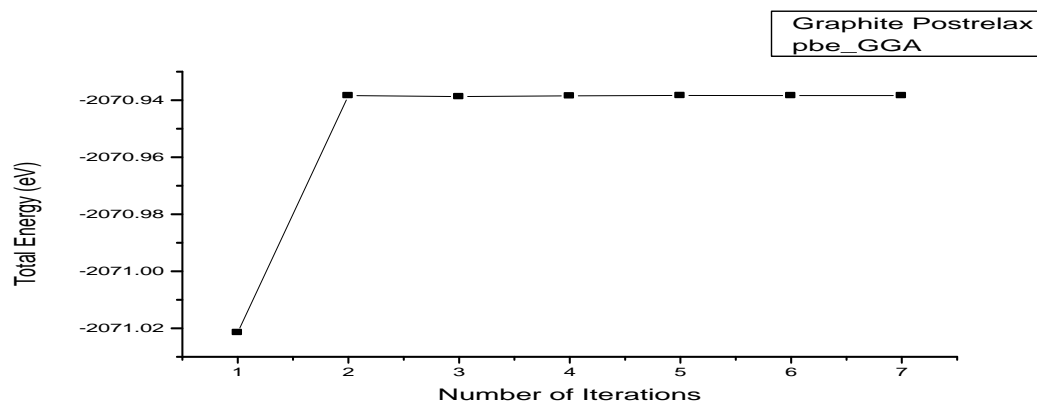


Fig. 4.5: Variations of Total Energy (eV) against Number of Iterations.

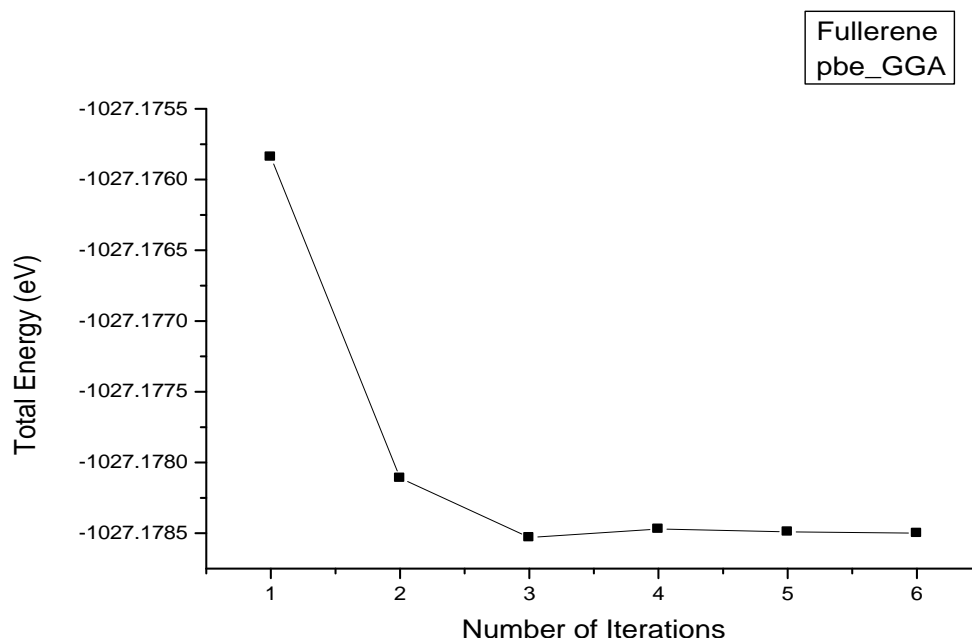


Fig. 4.6: Variations of Total Energy (eV) against Number of Iterations.

4. DISCUSSION

From table 4.1, it can be observed that pbe XC functional has the minimum ground state energy for diamond bulk structure. This is in agreement with theory, because pbe (GGA) is theoretically a better approximation to XC energy functional than the rest LDA and LSDA [8 and 9]. However, pw_Lda is a bit better approximation compared to pz_Lda. Similarly, comparing light and tight FHI-aims species_default settings for relaxed and postrelaxed computations, tight gives an efficient and accurate converged ground state energies than the light settings. This is a good indication that diamond crystalline structure has been well optimized in the relaxed/postrelaxed FHI-aims computations.

The binding curve in Fig. 4.1 shows that the total energy of the bulk crystal of diamond increases as the number of iteration increases and converges steadily. The resulting binding curve indicates a stable total energy and also the best converged energy of -2072.56851605 eV for diamond. This variation pattern for diamond total energy against the number of iterations was found to be the same for the remaining XC functionals used in this study.

Fig. 4.2 and Fig. 4.3 also illustrate the variations of diamond's ground state energies against the number of iterations. It is clear that the graphs variations are almost the same, except that the total

energies values are different. In Fig. 4.2 graph, the total energy value increases steadily from the 1st iteration to the 2nd iteration, from where this value decreases a bit and is later maintained until convergence is reached. However, fig. 4.3 shows a slight different trend. The total energy value rather increases in the third iteration, this value was maintained until convergence was obtained. The resulting binding curve in Fig. 4.3 indicates a stable total energy and also the best converged energy of -2056.89840811eV for diamond.

From table 4.2, it can be observe that pbe XC functional also has the minimum ground state energy for graphite bulk structure. This is in agreement with theory, because pbe (GGA) is theoretically a better approximation to XC energy than the rest pw_lda and pz_lda [9]. However, pw_lda is slightly a better approximation when compared to pz_lda. Similarly, comparing light and tight species_default settings for relaxed and postrelaxed computations, tight gives an efficient and accurate converged ground state energies than the light settings. This is also a good indication that graphite crystalline structure has been well optimized in the relaxed/postrelaxed FHI-aims computations.

Fig. 4.4 and Fig. 4.5 illustrate the variations of ground state energies against number of iterations for graphite bulk structure. The trend in both Figures increases upwardly to create a curve pattern until it reaches stability at the 3rd, 4th, 5th, 6th and 7th iterations, this can be attributed to the covalent bonding and simple planar hexagonal stacking that exist in the bulk atom of graphite [10]. The resulting binding curve in Fig. 4.5 indicates a stable total energy and also the best converged energy of -2070.93836837 eV for graphite.

For Fullerenes, ground state energies for relaxed/postrelaxed computations was not successful, because FHI-aims could not write out the geometry.in_next_step file let alone post relax processing.

We suggest this could be due to the dimension of fullerenes lattice constant of 14.17 \AA , physical settings used and/or its spherical shape. However, we computed the ground state energies for light/tight settings without structure optimization. Table 4.3 shows fullerenes ground state energies for the three XC functionals using light/tight default settings. The table also shows that, tight default settings gives a more accurate converged minimum ground state energy when compared to the light default settings. This is in good agreement with the theory behind FHI-aims code that for “final” results (meV-level converged energy differences between large molecular structures, etc.), any results from the light level should be verified with more accurate post processing calculations using tight [6]. Also looking at the XC functional total energy values, it is obvious that pbe gives the minimum ground state

energy follow by pw_lda and then pz_lda. Hence, in accordance with theory pbe is much better in approximating the XC energy functional than pw_lda and pz_lda [8 and 9].

Figure 4.6 illustrates the variations of Fullerenes ground state energies for the pbe XC functionals against number of iterations. The trend in Fig. 4.6 decreases downwardly to create a curve pattern until it becomes stable at the 4th, 5th and 6th iterations, this can be attributed to the covalent bonding and spherical shape that exist in the bulk atom of fullerenes [10 and 11].

In this paper, we find out that all the three variants of the total energy from FHI-aims output file are the same for diamond structure but are all different in the case of graphite and fullerenes. This shows that fullerenes and graphite have narrow and zero HOMO-LUMO gap respectively, while diamond has a wide HOMO-LUMO gap. These results are in good agreement with experimental and theoretical literatures [10 and 12]. Tables 4.4-4.6 show estimated values for lowest unoccupied state (CBM), highest occupied state (VBM), overall HOMO-LUMO gap and smallest direct gap for diamond, graphite and fullerenes as obtained from the three XC functionals used in this study.

From table 4.4, using the estimated overall HOMO-LUMO gap, FHI-aims code predicted that diamond appears to be an indirect band gap. This agrees well with the report of Fleming *et al*, 1992. The smallest direct gap of 5.57611325eV for pbe_GGA is in good agreement with theoretical and experimental values [10 and 11] with a percentage error of 1.43%. According to FHI-aims output file, since the gap value is above 0.2eV, the system is most likely an insulator or a semiconductor. This FHI-aims output file comment agrees exactly with theoretical and experimental data. Diamond was characterized in many literatures to be an insulator [4], however, it was also considered as an indirect wide band gap semiconductor [1] that is suitable for high temperature electronic applications. The rest XC functionals pw_lda and pz_lda Smallest Direct Gap are also in good agreement with experimental values of 5.5eV [11] with 1.96% error.

From table 4.5, using the estimated overall HOMO-LUMO gap, FHI-aims predicted that graphite also appears to be an indirect band gap. The smallest direct gap of 0.21308645eV for pw_lda is in good agreement with theoretical and experimental values [10]. According to FHI-aims output file, since the HOMP-LUMO gap value (0.00072958eV) is rather small (approximately zero gap) and we use a finite k-point grid, the material is most likely metallic in the sense that there are states at or near the Fermi level. This FHI-aims output comment shows that graphite is a conductor, and it agrees exactly with theoretical and experimental data [13]. Also, the approximately zero gap value of FHI-aims output file

is in agreement with the literature [10]. The rest XC functionals pz_lda and pbe_GGA Smallest Direct Gap are also in good agreement with experimental values within small percentage errors.

From table 4.6, using the estimated overall HOMO-LUMO gap, FHI-aims predicted that fullerenes also appears to be an indirect band gap. The smallest direct gap of 8.21131432eV for pw_lda and the remaining XC functionals values do not agree with theoretical value of 1.83eV [12] and experimental value of 2.3eV [Byun 2012, PhD Dissertation, Pennsylvania State University]. According to FHI-aims output file, since the gap value is above 0.2 eV. The system is most likely an insulator or a semiconductor. This FHI-aims output prediction agrees exactly with theoretical and experimental data, Fullerenes was reported to be a band insulator, direct band-gap semiconductor [1]. In addition, fullerenes can be converted from a semiconductor into a conductor or even superconductor when doped with alkali metals [14]. The rest XC functionals pz_lda and pbe_GGA Smallest Direct Gap are also not in good agreement with theoretical and experimental values [12].

5. CONCLUSION

The total ground state energy and electronic band structure of Fullerenes (C_{60}) for University]. According to FHI-aims output file, since the gap value is 2 eV. The system is most likely an insulator or a semiconductor. This FHI-aims output prediction agrees exactly with theoretical and experimental data, Fullerenes was reported to be a band insulator, direct band-gap semiconductor above 0. [1]. In addition, fullerenes can be converted from a semiconductor into a conductor or even superconductor when doped with alkali metals [14]. FCC, Graphite for hcp and Diamond crystal were calculated using the local-density approximation (LDA) in the parameterization by [15-17], and PBE+vdW approach as defined by [18]. The results of the total energy required for binding/stability of the ground state during the optimized process were found to converge faster with the 12x12x12 k-grid points in the Brillouin zone of the FHI-aims code. Similarly, FHI-aims tight/postrelaxed settings were found to give more accurate converged results. In terms of the XC functionals, pbe_GGA was better in approximating the XC energy functional than LDA. The result presented above have confirmed a faster and more accurate prediction of the electronic band structure and total energies of solids considered when compared to literature report of other studies reporting similar band gaps and/or total energies. Major findings of this research are; Graphite is a zero gap conductor (0.00072958eV), diamond is a wide band gap semiconductor (5.57611325eV). These are in good agreement with experimental values of 0eV and 5.45eV, respectively. However, fullerenes is also a wide band gap semiconductor

(8.21131431eV). This band gap does not agree with what was obtainable in the literature (1.83eV and 2.3eV). This discrepancy might probably be due to the present DFT calculations of the solid fullerene's lattice constant, spherical shape and the optimized parameters used in the study. Conversely, Graphite is a suitable candidate for optoelectronic and other electronic devices. Diamond is suitable for high temperature thermal electronic devices, while fullerenes is a good material for conversion into conductors and superconductors.

REFERENCES

1. Pierson H. O.. *Handbook of Carbon, Graphite, Diamond and Fullerenes*. Noyes Publications, New Mexico; 1993.
2. Shunhong Z., Jian Z., Qian W., Xiaoshuang C., Yoshiyuki K., and Puru J., Penta- graphene: A new carbon allotrope . *PNAS*, 2014; 112(8): 2372–2377.
3. Larry A., Al Fasim M., Richard S.W., Francesco D., and Nicola M. Novamene: A new Class of Carbon Allotropes. *Materials Science, Chemistry, Heliyon* 3. 2017; 3(2): [DOI: 10.1016/j.heliyon.2017.e00242](https://doi.org/10.1016/j.heliyon.2017.e00242).
4. Adams W. and Williams L. *Nanotechnology Dymistified*. United States of America:Mcgraw Hill; 2007.
5. Patrizia C., Gerald G and A. M. Koster. First-Principle Calculations of Large Fullerenes. *Journal of Chemical Theory and Computation*. 2009; 5: 29-32.
6. Blum V., Gehrke R., Hanke F., Havu P., Havu V., Ren X., Reuter K., and Matthias S. *Ab Initio* Molecular Simulations with Numeric Atom-Centered Orbitals. *Comp. Phys. Commun*. 2009; 180 (11): 2175–2196.
7. Viktor A., Oliver H., and Sergey L. *Hands-On Tutorial on Ab Initio Molecular Simulations, Tutorial I: Basics of Electronic-Structure Theory*. Berlin, Fritz-Haber-Institut der Max-Planck-Gesellschaft. 2011.
8. Parr, R. G. and Yang, W. *Density-Functional Theory of Atoms and Molecules*. Oxford University Press: New York. 1989.
9. Fiolhais C., F. Nogueira, and M. Marques (Eds.) *A Primer in Density Functional Theory*. Vol. 620, Springer-Verlag, Berlin. 2003.

- 260 10. *Krueger A.* Carbon Materials and Nanotechnology. WILEY-VCH Verlag GmbH & Co. KGaA,
261 Weinheim. 2010.
- 262 11. Fleming R. M., B. Hessen, T. Siegrist, A. R. Kortan, P. Marsh, R. Tycko, G. Dabbagh, and R.
263 C. Haddon, Fullerenes: Synthesis, Properties, and Chemistry, Chapter 2: Crystalline
264 Fullerenes. AT&T Bell Laboratories, Murray Hill, NJ 07974. 1992.
- 265 12. Heggie M. I., M. Terrones, B. R. Eggen, G. Jungnickel, R. Jones, C. D. Latham, P. R. Briddon
266 and H. Terrones. Quantitative Density Functional Study of Nested Fullerenes. *Physical*
267 *Review B, Condensed Matter and Materials Physics*. 1998; 57(21): 13339-13342.
- 268 13. Charlier J.-C. X. Gonze and J.-P. Michenaud. First-Principles Study of the Stacking
269 Effect on the Electronic Properties of Graphite(S) . *Carbon*. 1994; *Vol. 32, No. 2*:
270 289-299.
- 271 14. *Katz, E. A.* *Fullerene Thin Films as Photovoltaic Material*. In *Sōga, Tetsuo*. Nanostructured
272 materials for solar energy conversion. *Elsevier*. 2006; 361–443. *ISBN 978-0-444-52844-5*.
- 273 15. Perdew, J.P. and Wang, Y. Accurate and Simple Analytic Representation of the Electron-Gas
274 Correlation Energy. *Physical Review B*, 1992; 45(23): 13244-13249.
275 <http://dx.doi.org/10.1103/PhysRevB.45.13244>.
- 276 16. Perdew, J.P. and Zunger, A. Self-Interaction Correction to Density-Functional Approximations
277 for Many-Electron Systems. *Physical Review B*. 1981; **23**, 5048-5079.
278 <http://dx.doi.org/10.1103/PhysRevB.23.5048>.
- 279 17. Perdew J. P., K. Burke, and M. Ernzerhof. Generalized gradient approximation made simple.
280 *Phys. Rev. Letter*. 1997; 77 (18): 3865–3868..
- 281 18. Tkatchenko A. and M. Scheffler. Accurate molecular van der Waals interactions from ground
282 state electron density and free-atom reference data. *Physical review letters*. 2009; 102(7),
283 073005. [DOI: 10.1103/PhysRevLett.102.073005](https://doi.org/10.1103/PhysRevLett.102.073005).